JOURNAL OF MATERIALS SCIENCE **36** (2001) 5609–5624

Ceramic joining IV. effects of processing conditions on the properties of alumina joined via Cu/Nb/Cu interlayers

R. A. MARKS, J. D. SUGAR, A. M. GLAESER
Department of Materials Science and Engineering, University of California, CA, USA; Center for Advanced Materials, Lawrence Berkeley National Laboratory, Berkeley, CA 94720, USA
E-mail: aglaeser@sapphire.berkeley.edu

Multilayer copper/niobium/copper interlayers consisting of 3 μm thick cladding layers of copper on a 125 μm thick niobium core layer were used to join aluminum oxides at 1150°C or 1400°C, or both. Three microstructurally distinct aluminum oxides were joined—a 25 μm grain size 99.5% pure alumina, a submicron grain size 99.9% pure alumina, and single crystal sapphire. Two-phase interlayer microstructures containing both copper-rich and niobium-rich phases developed during bonding. In some cases, the initially continuous copper film evolved via Rayleigh instabilities into an array of discrete copper-rich particles along the interlayer/alumina interface with concurrent increases in the niobium/alumina contact area. Processing conditions (temperature and applied load) and the alumina microstructure (grain size) impacted the extent of film breakup, the morphologies of the copper-rich and niobium-rich phases, the interlayer/alumina interfacial microstructure, and thereby the strength characteristics. Joints possessing a large copper/alumina interfacial area fraction were comparatively weak. Increases in bonding pressure and especially bonding temperature yielded interfaces with higher fractional niobium/alumina contact area. For joined polycrystals, such microstructures resulted in higher and more consistent room temperature fracture strengths. Joined 99.9% alumina polycrystals retained strengths >200 MPa to 1200°C. Relationships between processing conditions, interlayer and ceramic microstructure, and joint strength are discussed. © *2001 Kluwer Academic Publishers*

1. Introduction

Advances in processing science and manufacturing continue to improve the properties of both structural and electronic ceramics. However, the practical use of ceramics often requires that they be intimately connected, i.e., chemically bonded, to other ceramic or metal components. Joining constitutes an important aspect of processing ceramic-based and ceramic-containing assemblies and devices. Producing metal/ceramic joints with reproducibly good properties is thus technologically important.

Diffusion bonding and brazing are two established routes to joining ceramic components by means of metallic interlayers [see, for example, 1–5]. Diffusion bonding is well suited to forming refractory joints. However, meticulous surface preparation, high applied loads, and prolonged periods at high temperatures (potentially exceeding the desired application temperature) are often necessary to form reliable diffusion-bonded joints. In contrast, brazing generally requires clean but not polished surfaces and more modest loads; these characteristics, coupled with a short process time, make this method more attractive for mass production. The fabrication of brazed joints suitable for *high-temperature* applications requires the development of refractory brazes. Attempts at brazing with pure nonreactive high melting point metals (e.g., platinum) have been unsuccessful [6]. Reactive metal additions to a braze produce more favorable wetting behavior, and can improve joint properties, however, such additions are not a panacea. Since high service temperatures require even higher brazing temperatures, undesirable chemical reactions between the braze and the components to be joined, as well as deleterious chemical and microstructural changes in the joined components become increasingly difficult to avoid. Therefore, the development of techniques for joining ceramics *at or below* their intended service temperature has been of great interest.

Partial transient liquid phase (PTLP) bonding [7–17] produces refractory joints at relatively low temperatures. The process is essentially an extension of the solid-liquid interdiffusion (SLID) and transient liquid phase (TLP^{TM}) techniques developed by Bernstein and Bartholomew [18] and Duvall *et al*. [19], respectively. The current study applies a variant of the PTLP method to the joining of alumina via copper/niobium/copper interlayers. Prior work [10, 17] has shown that strong

joints can indeed be fabricated by this technique. The present study clarifies the mechanism of joint formation. The effects of processing conditions (temperature, applied load, and ambient atmosphere) and alumina characteristics (grain size, purity) on the interlayer/ceramic interfacial microstructure are described, and the resulting microstructural differences are related to differences in room-temperature and/or high-temperature fracture behavior.

2. Background

The current bonding approach uses a multilayer metallic interlayer. Both of the ceramic surfaces to be joined are coated with a thin cladding layer of a low melting point metal, copper in this case. A thicker core layer of a high melting point metal, niobium in this study, is inserted between the coated surfaces. The bonding temperature used, 1150°C or 1400°C, is such that the cladding layers melt, while the core layer remains solid. Consequently, the wetting behavior of the liquid (copper) on the ceramic (alumina) and core layer (niobium) is of interest. Additionally, since the solubility of copper in niobium is limited [20], a two-phase metallic microstructure persists within the interlayer, and both copper/alumina and niobium/alumina contact regions can develop at the metal/ceramic interface. Properties (e.g., strength and effects of impurities) of the copper/alumina and niobium/alumina interfaces are thus also important. Studies addressing these issues (wetting and interfacial properties) are briefly reviewed here; complementary discussions can be found in prior publications [17, 21].

2.1. Prior work on niobium/alumina interfaces

2.1.1. Interface fabrication

Niobium/alumina interfaces can be generated by internal oxidation of aluminum-niobium alloys [22, 23], and also by the deposition of niobium overlayers onto sapphire [24–29]. Interfaces produced by these methods exhibit preferred misorientation relationships. In some cases, the close-packed (110) planes of niobium align parallel to the close-packed (0001) oxygen planes in alumina, while in other instances, misorientation relationships that result in good lattice matching at the interface develop. Such preferred misorientation relationships have been duplicated by diffusion bonding suitably misoriented single crystals of niobium and sapphire; other misorientation and boundary plane orientations have also been produced by diffusion bonding. The use of polycrystalline niobium, alumina, or both can be employed to further expand the misorientation range sampled. Collectively, such samples have been used to examine the strength and fracture characteristics [28, 30–37], bonding mechanisms [25, 29, 31, 38–43], and interfacial structure [22–24, 26–28, 38–40, 44–46] of niobium/alumina interfaces.

Diffusion bonding has been the most common method of interface fabrication. Bonding temperatures have ranged from 920°C to 1950°C and applied loads from 2 MPa to 16 MPa. Successful joining at temperatures below ≈1400°C generally requires sputter-cleaning of the well-polished surfaces, and the use of ultrahigh vacuum (UHV; $\approx 10^{-8}$ Pa) conditions. In the initial stages of diffusion bonding, niobium/alumina interfacial area is increased by plastic deformation of the metal (and sometimes the ceramic). At temperatures above ≈1700°C, substantial dissolution of alumina in niobium occurs [47], and reprecipitation of alumina at interfacial voids during cooling can contribute to flaw elimination [38–42]. At more modest temperatures (e.g., ≈1450°C), work by Reimanis [43] indicates that void removal at niobium/sapphire interfaces is rate-limited by niobium volume diffusion, and is thus sluggish; void removal was incomplete even after 18 h at ≈1450°C.

2.1.2. Interface characterization

Rühle, Mader, and coworkers [22, 23, 26, 38–40, 44–46] have used high resolution transmission electron microscopy (HRTEM) to determine the structure and chemistry of niobium/sapphire interfaces. Interfaces in which $(110)_{\mathrm{Nb}} \| (0001)_{\mathrm{Sapphire}}$, or those that exhibit good lattice matching have been studied. The special interfaces examined are coherent, with periodic misfit dislocations located at a stand-off distance from the interface. Knauss and Mader [46] and Ohuchi [25, 29] have investigated whether aluminum or oxygen composes the terminating layer in alumina at the niobium/alumina interface; the results suggest that the termination depends on the experimental conditions.

2.1.3. Work of adhesion and fracture energies

The work of adhesion, W_{AD}, is often defined as the energy required to cleave (and thus remove) an interface, and to produce two free surfaces. The interface and surface energies are amenable to calculation, and thus, first-principles calculations have provided estimates of W_{AD}. The value of W_{AD} will depend upon the crystallographic details of the interface and surfaces, but also on whether the interface and surface structures are allowed to relax to equilibrium. Equilibrium with the ambient environment is also an important consideration; Saiz *et al*. [48, 49] have pointed out the potential for oxygen partial pressure (p_{O_2}) effects on interfacial energies*, and thus, on W_{AD} in metal/alumina systems. Batirev *et al*. [51] use the term (mechanical) work of separation, W_{SEP}, to consider situations in which, for example, relaxation or equilibration of the surface structure does not occur.

Several recent first-principles calculations [51–53] have focussed on assessing the structure and energy of the coherent $(111)_{\mathrm{Nb}} \| (0001)_{\mathrm{Sapphire}}$ niobium/sapphire interface. Particular attention has been given to determining whether the sapphire is terminated by aluminum (as is predicted for sapphire/vapor interfaces over a

*A recent study of equilibrium shapes of magnesia particles in a copper matrix that has been equilibrated with a wide range of ambient oxygen partial pressure provides clear evidence that interfacial energies in a solid-metal–metal-oxide system depend on the oxygen potential [50].

wide range of oxygen partial pressure [54]) or is terminated by oxygen (as suggested by experimental work). The calculations indicate that at equilibrium the terminating plane hinges on the ambient oxygen partial pressure (po_2). Since W_{AD} for an aluminum-terminated surface (stable at low po_2) is roughly one-fourth the value for an oxygen-terminated interface, substantial changes in the work of adhesion (or the work of separation) could be induced by changes in the ambient oxygen potential [51, 53]. Depending upon the exact position of the cleavage plane, and whether or not the surfaces created by fracture are allowed to relax, values of W_{SEP} ranging from 2.8 to 9.8 J/m^2 are predicted [52]. A more recent and refined calculation by Zhang and Smith [53] suggests values for W_{SEP} of 2.6 and 10.6 J/m^2 for cleavage of aluminum-terminated and oxygen-terminated niobium/alumina interfaces, respectively.

The work of adhesion provides a lower bound on the work of fracture. As a result, one can anticipate that the fracture energy will exceed the work of adhesion unless experiments are designed to minimize the contributions of plastic dissipation. Spallation experiments in which plasticity effects were minimized indicate a fracture energy of 0.6–0.8 J/m^2 for $(111)_{Nb}\|(0001)_{Sapphire}$ interfaces [28]. However, more generally, reported fracture energies are substantially higher than computed W_{AD} values. In the niobium/sapphire system the fracture energy depends upon the relative misorientation of the niobium and sapphire, the orientation of the niobium/sapphire interface plane, the crack propagation direction, and the processing conditions (time, temperature, pressure) [32–37, 55]. Fracture energies as high as $\approx$2400 J/m^2 have been reported for niobium/sapphire interfaces with $(110)_{Nb}\|(0001)_{Sapphire}$ [33, 36, 37], while other orientation pairs exhibit fracture energies as low as $\approx$60 J/m^2 [32, 33, 35–37]. The introduction of polycrystalline niobium foils or polycrystalline alumina will decrease the prevalence of such favored misorientation relationships. For example, polycrystalline niobium/sapphire couples have fracture energies in the vicinity of $\approx$60 J/m^2, as only a small fraction of niobium grains are likely to be oriented such that the interfaces have high fracture energy [32]. However, all of these values are much larger than W_{AD} , and it has been proposed that the work of fracture is proportional to W_{AD}^n where $n > 1$ [56].

The microchemical and microstructural characteristics of the niobium and the alumina used can also impact the fracture energies and fracture path. Impurities in the metal or in the ceramic, or impurities intentionally introduced on the bonding surfaces by sputter-deposition can have beneficial or deleterious effects on the fracture energy. Sputter cleaning and UHV diffusion bonding at 1000–1200°C produces interfaces having a fracture energy close to that obtained from conventional high vacuum diffusion bonding (>1400°C, no sputter cleaning). Titanium increases the fracture energy while silver decreases the fracture energy [35, 36]. The use of "weaker" aluminas will tend to shift the fracture path to the ceramic [30]; impurities in the ceramic such as silicates may introduce silicon into the interlayer, embrittling it, and promoting failure within the metal layer [30, 57].

Fracture strengths depend upon the test method, the sample size, and are sensitive to the flaw population. Klomp [58] reports that Elssner and Krohn [57] prepared diffusion bonded joints at 1300°C, 1400°C, and 1600°C with room-temperature strengths of 259 MPa, 198 MPa, and 365 MPa, respectively, suggesting "strong" joints can be fabricated. Morozumi *et al.* [31] diffusion-bonded sapphire between two niobium polycrystals at 1500–1800°C. Tensile tests performed on these joints revealed an average strength of 120 MPa at room temperature. Strengths near 100 MPa were maintained up to $\approx$900°C, but fell to $\approx$35 MPa at 1000°C and $\approx$15 MPa at 1600°C. Extensive plastic deformation of the niobium was noted at the highest test temperatures.

2.2. Prior work on copper/alumina interfaces

2.2.1. Interface fabrication

Paralleling the work on niobium/alumina, copper/alumina interfaces have been produced by internal oxidation of copper-aluminum alloys [59], by deposition processes [e.g., 29, 60, 61–67], and by diffusion bonding [55, 68–75]. Several studies on copper/alumina interfaces have shown that interfaces in which (111) copper is parallel to the (0001) close-packed oxygen planes in alumina are preferentially formed [59, 60, 63, 66–68] and prompted the production of crystallographically similar interfaces by diffusion bonding [75].

2.2.2. Interface characterization

High-resolution TEM studies of $(111)_{Cu}\|(0001)_{Sapphire}$ interfaces generated by either internal oxidation [59] or by diffusion bonding [75] have been performed. However, unlike niobium/alumina interfaces, TEM observations found even these special interfaces to be incoherent [59, 75]. Photoemission spectra [61] indicate that copper interacts weakly with alumina; the spectra are consistent with the proposal that copper bonds to the oxygen atoms on the alumina surface [62].

2.2.3. Work of adhesion and fracture energies

Solid-copper/alumina interfaces have been the subject of theoretical study [62, 76]. Calculations by Zhao *et al.* [76] suggest $W_{AD} \approx 0.9$ J/m^2 for the $(111)_{Cu}\|(0001)_{Sapphire}$ interface. This result is in reasonable agreement with experimental values [60, 67][†]. (If an *unrelaxed* (0001) sapphire surface is formed, W_{SEP} is 2.9 J/m^2.) We note that these values of the work of adhesion for copper/alumina interfaces lie below those indicated for niobium/alumina interfaces.

[†] By assessing the equilibrium shape of solid droplets of copper on (0001) alumina substrates, the work of adhesion can be calculated from the droplet geometry.

As was the case for both niobium/sapphire interfaces, the work of fracture for copper/sapphire interfaces is substantially higher than W_{AD}. For copper/sapphire interfaces, the work of fracture is strongly affected by oxygen impurities. Studies by Rühle *et al.* [75] indicate fracture energies for $(111)_{Cu}\|(0001)_{Sapphire}$ interfaces of the order of 150–200 J/m^2 when the copper is "pure" versus 500–1350 J/m^2 for copper containing 60 ppm dissolved oxygen. Studies by Reimanis and coworkers also show effects of oxygen content on interfacial microstructure [73] and fracture energies [77]. Diffusion bonding under a rather modest vacuum, and thus, a potentially high ambient p_{O_2} has produced joints with an average bend strength of 177 ± 13 MPa [74].

2.3. Wetting studies

In order for a liquid to flow into and fill gaps between two parallel solid surfaces, the condition $\theta_{LC} + \theta_{LM} < 180°$ must be met, where θ_{LC} and θ_{LM} are the contact angles of the liquid on the ceramic and on the metal core, respectively. If the surfaces are rough and locally diverge, then a lower contact angle sum is required to fill gaps. Unfilled gaps become interfacial defects or flaws that can limit the strength of the interface and serve as failure initiation sites. As a result, the wetting behavior of copper on both alumina and niobium is of interest.

The effects of oxygen on the wettability of liquid copper on alumina have been examined [69, 78–81], and studies consistently reveal that θ_{LC} is reduced at higher ambient p_{O_2}. For "pure" copper on alumina, contact angles in the range of 120–140° are typical in the low p_{O_2} range. The oxygen activities associated with $\theta_{LC} < 120°$ are far greater than those believed to be present in the current study, and thus other additives that lower θ_{LC}, or a sufficiently low θ_{LM} are vital to successful bonding.

The addition of metals such as titanium or chromium to copper can significantly reduce its contact angle on alumina. In the case of titanium, the reduction occurs by formation of a thin reaction layer at the copper/alumina interface [82, 83], i.e., reactive wetting. For chromium, the contact angle reduction has been attributed to the segregation of metal-oxygen clusters (CrO) to the copper/alumina interface [84]. Niobium additions also reduce θ_{LC} of copper on alumina [12, 85]; however, the mechanism by which this reduction occurs is not known. Nakashima and coworkers [12] examined the wetting behavior at 1150°C of copper containing 2 wt% niobium on alumina under low ambient p_{O_2} conditions ($p_{O_2} \approx 10^{-22}$ atm). Upon heating to 1150°C, the copper-rich liquid exhibited a lower *initial* contact angle (105°) than "pure" copper on alumina (≈125°) at 1150°C [12]. In contrast to pure copper, the contact angle of the copper-niobium alloy decreased with increasing time, reaching values <20° after 5 h at 1150°C. At higher temperatures (e.g., 1400°C) this reduction in θ_{LC} is likely to occur more rapidly. The temperature dependence of θ_{LC} is not known. The temperature trends of *pure* copper [86–88] and other metals on oxides [89] would suggest a decrease in θ_{LC} as temperature increases, however, the temperature dependence of segregation and its impact on surface and interface energies must also be considered.

The contact angle of copper on niobium decreases significantly as the temperature is increased, from ≈67° at 1090°C [90] to <2° at 1500°C [91]. The work of De Lima *et al.* [90] indicates that contact angles for copper on niobium increase as the oxygen content of the niobium increases. Sessile drop measurements by Nakashima [12] evaluated the wetting of 99.999% pure copper on 99.99% pure niobium foil at 1150°C in vacuum. The results indicated an initial contact angle of 67°, which decreased to ≈40° in 5–10 min, and decreased more slowly to ≈28° after 4 h at 1150°C. If the time-dependence of the contact angle formed by copper-rich copper-niobium alloys is due to progressive dissolution of niobium, then with increasing time, an increasing fraction of interfacial defects should be removed provided liquid redistribution is possible. At higher temperatures, where the contact angle sum is much lower and more rapid dissolution is expected, liquid redistribution and flaw filling should occur more rapidly.

2.4. Prior work on alumina joined with Cu/Nb/Cu interlayers

Shalz *et al.* [10] found that strong (181 ± 45 MPa) alumina joints could be prepared using multilayer copper/niobium/copper interlayers by processing in a molybdenum hot press at 1150°C using a 5.1 MPa applied load. In contrast, Marks *et al.* [17] found when joints were prepared in a graphite hot press at 1150°C with a 2.2 MPa load, the strength decreased dramatically. Samples that survived beam preparation and were tested had an "average" strength of only 78 MPa and a standard deviation of ±22 MPa, however, these figures overestimate the strength and underestimate the scatter. For both joints, failures occurred primarily along the alumina/interlayer interface. Initially, it was believed this strength difference might reflect the very different ambient p_{O_2} in the two hot presses used and its impact on the wettability of liquid copper on alumina and niobium[‡].

Effects of ambient p_{O_2} were suggested when samples were subjected to post-bonding anneals [17]. A modest strength decrease and an increased fraction of interfacial failures followed ≈200 h anneals at 1000°C in low p_{O_2}, gettered-argon; vacuum anneals of similar duration at 1000°C had no obvious effect on strength and failure characteristics.

Bonding temperature had an important effect on joint characteristics [17]. Assemblies produced in a graphite environment at ≈1400°C with a 2.2 MPa applied load had an average strength of 241 ± 18 MPa, and ≈75% of the 42 beams tested failed in the ceramic. Ceramic failures continued to be observed in high-temperature fracture tests performed up to 1100°C, suggesting a

[‡] The ambient p_{O_2} in the graphite hot press is expected to be significantly lower than that in the molybdenum hot press. Saiz *et al.* [92] have shown that copper containing oxygen has a lower contact angle on niobium than 99.999% pure copper.

strong interface was produced. The fracture energy and fatigue properties of joints produced under these conditions are currently being examined by Kruzic *et al.* [93].

3. Experimental procedures

3.1. Materials

Blocks of a 99.5% pure, ≥98% dense alumina (AD995, Coors Technical Ceramics Co., Oak Ridge, TN) were used for joints processed at 1150°C. Blocks of a higher strength 99.9% pure, ≥98% dense alumina (SSA-999W, Nikkato Corp., Osaka, Japan) were used for one of the joints processed at 1400°C, while cylindrical sapphire plugs (Insaco Inc., Quakertown, PA) were used for the other. The joining surfaces of the polycrystalline alumina substrates were ground flat with a surface grinder and lapped (1–2 h) with progressively finer diamond suspensions (South Bay Technologies, San Clemente, CA). After polishing with 6 μm, 3 μm and 1 μm diamond media, the final polish entailed lapping with colloidal silica (Struers, Westlake, OH) on a polyurethane plate. The circular (0001) faces of the sapphire plugs had an optical finish, and required no further polishing. Samples to investigate interfacial microstructure evolution were fabricated using ≈0.5 mm thick, high-purity, optical finish, *c*-axis (±≈1°) sapphire substrates (Meller Optics Inc., Providence, RI) that also required no additional polishing.

A 125 μm thick (99.99% pure) niobium foil (Goodfellow, Berwyn, PA) was cut to the size of the joining surface for each experiment. A commercial wire (Consolidated Companies Wire and Associated, Chicago, IL) served as the copper source. The copper and niobium sources are the same as those used in previous experiments by Shalz *et al.* [10] and Marks *et al.* [17, 21], and were prepared using the same procedures employed previously.

3.2. Coating procedure

The alumina substrates were cleaned in an ultrasonic bath using a variety of solvents (soap and water, distilled water, acetone, and isopropyl alcohol) prior to annealing in air (≈1000°C for 1 h) to burn off any organics remaining from the cleaning solutions. Copper wire was cut into small pieces and cleaned in isopropyl alcohol. The pieces were then bright-dipped in a nitric acid : water (5 : 1) solution for 5–10 s. Immediately after bright-dipping, the copper was rinsed in distilled water and left to soak in isopropyl alcohol. Prior to loading the copper into the deposition system, it was rinsed in nanopure water (≥18 MΩ · cm) and dried with hot air. The annealed substrates were then placed inside the deposition chamber, and the copper was placed in tungsten wire baskets approximately 3–7 cm above the substrates. After the chamber evacuated to 2.5×10^{-4} Pa, the copper was heated until it melted. During heating and evaporation, the chamber pressure typically rose to between 3×10^{-3} Pa and 3×10^{-2} Pa. The coated substrates were kept inside the vacuum chamber until joint assembly. The amount of copper evaporated was chosen to yield an ≈3 μm thick coating. Actual thicknesses are summarized in Table I.

3.3. Bonding conditions and hot press specifics

Niobium foils were degreased in water and detergent, ultrasonicated in isopropyl alcohol, rinsed in ethanol, then in nanopure water, and dried with hot air. The copper-coated alumina substrates were then removed from the vacuum chamber and loaded into a hot press with the niobium foil sandwiched between the coated surfaces. The joints were processed under vacuum (≈10^{-2} Pa) in either a molybdenum element/molybdenum heating shield hot press with alumina furniture, or a graphite element/graphite shield hot press with graphite furniture. Table I summarizes the processing conditions for each joint, and notes any interruptions (holds) in the heating cycle needed to maintain a vacuum below ≈10^{-2} Pa. Assemblies were heated at 4°C/min, soaked at the bonding temperature (1150°C or 1400°C) for 6 h, and cooled at 2°C/min.

TABLE I Processing conditions and average copper thickness for copper/niobium/copper joints

Substrate	Coating thickness (μm)	Joining temperature (°C)	Hot press	Applied load (MPa)	Interruptions (Holds) (°C-min)
99.5% Alumina	3.0	1150	Molybdenum	6.8–8.2[b]	None
99.5% Alumina	3.0	1144	Graphite	2.2	None
99.5% Alumina	1.9–3.2[a]	1150	Graphite	7.5	None
Sapphire window	1.7–3.6[a]	1150	Graphite	1.6	None
Sapphire plugs	3.9	1382	Graphite	1.9	1153–30 1288–60 1369–15
99.9%Alumina	2.9	1382	Graphite	2.3	None

[a]The thickness has been measured using both profilometry and mass gain techniques. The profilometry measurements reveal variations in the copper thickness; the coating is thicker on the portion of the substrate placed closer to the center of the deposition chamber. In cases where both mass gain and profilometry measurements have been made, the average thickness determined by mass gain has been closer to the higher values from profilometry measurements. It is expected that the average copper thickness in these two joints deviates from 3.0 μm by 0.5 μm at worst since the same amount of copper is evaporated in each coating run. See reference [21] for further details on these measurements.

[b]The applied load in the molybdenum hot press is controlled manually with a hydraulic jack. Due to thermal expansion in the hot press column during heating, the applied load increases and is manually released. Consequently, the applied load fluctuates between the stated values, but an average load of 7.5 MPa is maintained.

3.4. Beam preparation

Each bonded assembly was machined into 2 cm × 4 cm × 3 mm plates. One of the 2 cm × 4 cm surfaces was ground flat and polished to a 1 μm finish. The 99.5% alumina plates were successively polished with 15 μm, 6 μm, and 1 μm diamond paste on a vibratory polisher. The polishing of 99.9% alumina and sapphire plates used the same lapping technique as for joining surface preparation. Each plate was subsequently machined into beams of ≈3 mm × ≈3 mm cross-section. Both ≈4 cm-long edges of each beam were bevelled on a metal grinding wheel impregnated with 6 μm diamond abrasive. The polished and bevelled side of each beam served as the tension face in mechanical testing. For the sapphire joint, additional polishing was done on the sides adjacent to the tensile face to remove flaws introduced during machining.

3.5. Mechanical testing

Prior to mechanical testing, beams were ultrasonically cleaned in ethanol and blown dry with hot air; this removed excess water from pores in the ceramic. The beams were loaded in a four-point bend test jig such that the interlayer (niobium) was at the center of the inner span (9 mm); the outer span was 25 mm. A flat crosshead was then lowered until it nearly contacted the jig, and was subsequently lowered at 50 μm/min until the beam fractured.

Strength measurements at elevated temperature were performed in a similar manner to room-temperature tests. A graphite jig with the same span dimensions and a displacement rate of 60 μm/min were used. The sample and jig were loaded into a flowing-argon atmosphere furnace with a graphite ram and tungsten heating elements and shields. The sample was held under a small constant load (equivalent to ≈9 MPa for the present sample dimensions) during heating so that displacements due to thermal expansion would not prematurely overload the beam, i.e., the system was under load control. The sample was heated at ≈10°C/min. When the testing temperature (800–1300°C) was reached, the system was held for 15–30 min prior to increasing the load (via displacement control) to allow thermal equilibration. Load/displacement data was obtained via a computer data acquisition system.

For both room-temperature and high-temperature tests, the stress was computed from the maximum load during testing (typically the load at fracture) using standard static loading analyses for monolithic materials. Fractures were characterized as either ceramic or interfacial failures based on visual inspection. Joints that failed along a metal/ceramic interface were further examined using an optical and/or a scanning electron microscope (SEM).

4. Results and discussion

4.1. Effect of ambient atmosphere and applied load on joint characteristics

Prior work [10, 17] using the 99.5% alumina indicated that significantly different strength characteristics and failure modes arose when the bonding environment, applied load, and temperature were changed. To verify the striking differences between joint properties obtained in bonds prepared at 1150°C in molybdenum versus graphite hot pressing environments, the original experiments were repeated. However, to minimize the possibility of inadvertent differences in processing, the materials for these two joints were prepared concurrently and subjected to identical polishing, cleaning, coating and assembly procedures. Both joints were then processed at 1150°C, one in the molybdenum hot press using a 7.5 MPa bonding load, the other in the graphite hot press using a 2.2 MPa load. Ideally, only the hot pressing environment and the applied load differ. After bonding, identical machining and polishing procedures were used to produce beams subjected to identical bend test conditions.

The failure probability versus joint strength characteristics of the two prior and the two new 99.5% alumina-based joints processed at 1150°C are shown in Fig. 1. Beams from the new joint processed in the molybdenum hot press and at higher load had an average fracture strength (205 MPa), a standard deviation in strength (±49 MPa), a strength range (120–275 MPa) that closely resembled those obtained in the prior experiment [10]. There was a higher incidence of ceramic (as opposed to interfacial) failure in the new joint, perhaps reflecting improved surface preparation procedures. When comparing these results to those for the new joint prepared in the graphite hot press, the average strength is somewhat higher (205 MPa versus 173 MPa), and the standard deviation is smaller (49 MPa versus 73 MPa). The most striking difference in the current set of bonds was in the *range* of strengths displayed: 69 to 290 MPa (graphite,

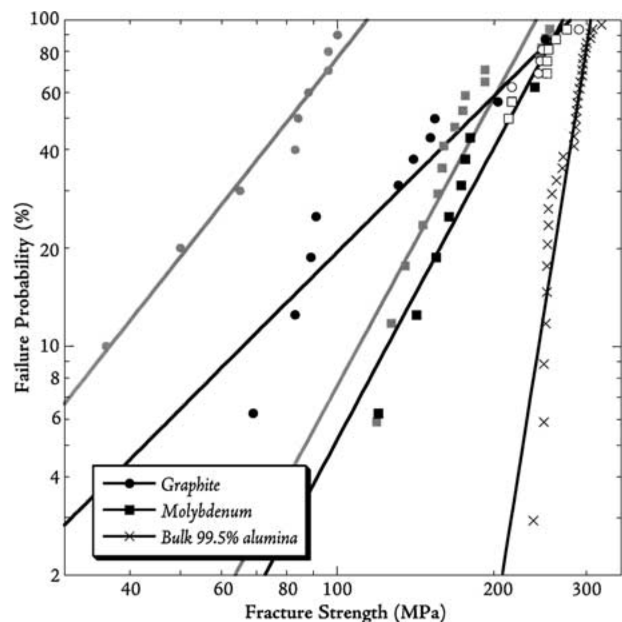

Figure 1 Failure probability plot comparing fracture strength of copper/niobium/copper joints processed under various conditions to the strength of bulk 99.5% alumina. Circles represent data from joints processed at 1150°C in a graphite hot press (2.2 MPa), while squares are for joints processed at 1150°C in a molybdenum hot press (7.5 MPa). Data sets in gray are from previous studies [10, 17] using similar processing conditions. Open symbols are for beams that failed in the ceramic rather than along the metal/ceramic interface.

2.2 MPa) compared to 120 to 275 MPa (molybdenum, 7.5 MPa). The relatively larger scatter and relatively lower strength for the bond prepared in a graphite environment and at lower load are consistent with prior findings [10, 17]. However, the difference in average strength indicated in the current set of bonds was much smaller than previously observed [§].

For both joints, most beams failed along the alumina/interlayer interface, but at stresses that varied over a relatively wide range; the few failures that originated and propagated entirely within the ceramic are denoted with open symbols in Fig. 1. Figs 2 and 3 show the metal side of beam fracture surfaces from the joints processed in the molybdenum and graphite hot presses, respectively. For each set of images, beams that spanned a range of fracture strength were selected. Each image within a set was taken at a region of the ceramic/interlayer interface along or near the beam tensile edge. The grain structure seen in all images is not of the niobium, but instead is the imprint of alumina grain boundary grooves on the metal. The prevalence of this imprint in all images indicates that the area fraction of ceramic/metal contact was high in all beams. This suggests that the observed strength differences were not caused by significant differences in area fraction of metal/ceramic contact.

In comparing the images in Fig. 2 with those in Fig. 3, it appears that the interfacial copper film (lighter phase) had broken-up more extensively and uniformly in bonds prepared in the molybdenum hot press (7.5 MPa). The variability in copper area fraction at the interface was much greater for bonds prepared in the graphite hot press (2.2 MPa); the variability in strength was also much greater in these bonds. Regions of essentially complete interfacial copper coverage (similar to that in Fig. 3a) were particularly evident in the weakest beams. (We note that the images in Figs 2 and 3 were taken in regions exhibiting the most extensive copper coverage near the tensile edge of beams.) Consequently, there appears to be some correlation between joint strength and extent of copper film among beams with the same processing history.

Differences in the interlayer/alumina microstructure are expected to cause differences in the fracture behavior. The relative area fractions of copper/alumina and niobium/alumina contact can have an impact because

[§] The coating method used makes it difficult to exactly duplicate the copper coating thickness. In the prior study [17], the copper layer for the bond prepared in the graphite hot press was somewhat thicker (3.8 μm) than in the current work (3.0 μm). As will be discussed, this thickness difference may be important in determining the ultimate interfacial microstructure and joint strength properties. Systematic studies of copper coating thickness effects are in progress [94].

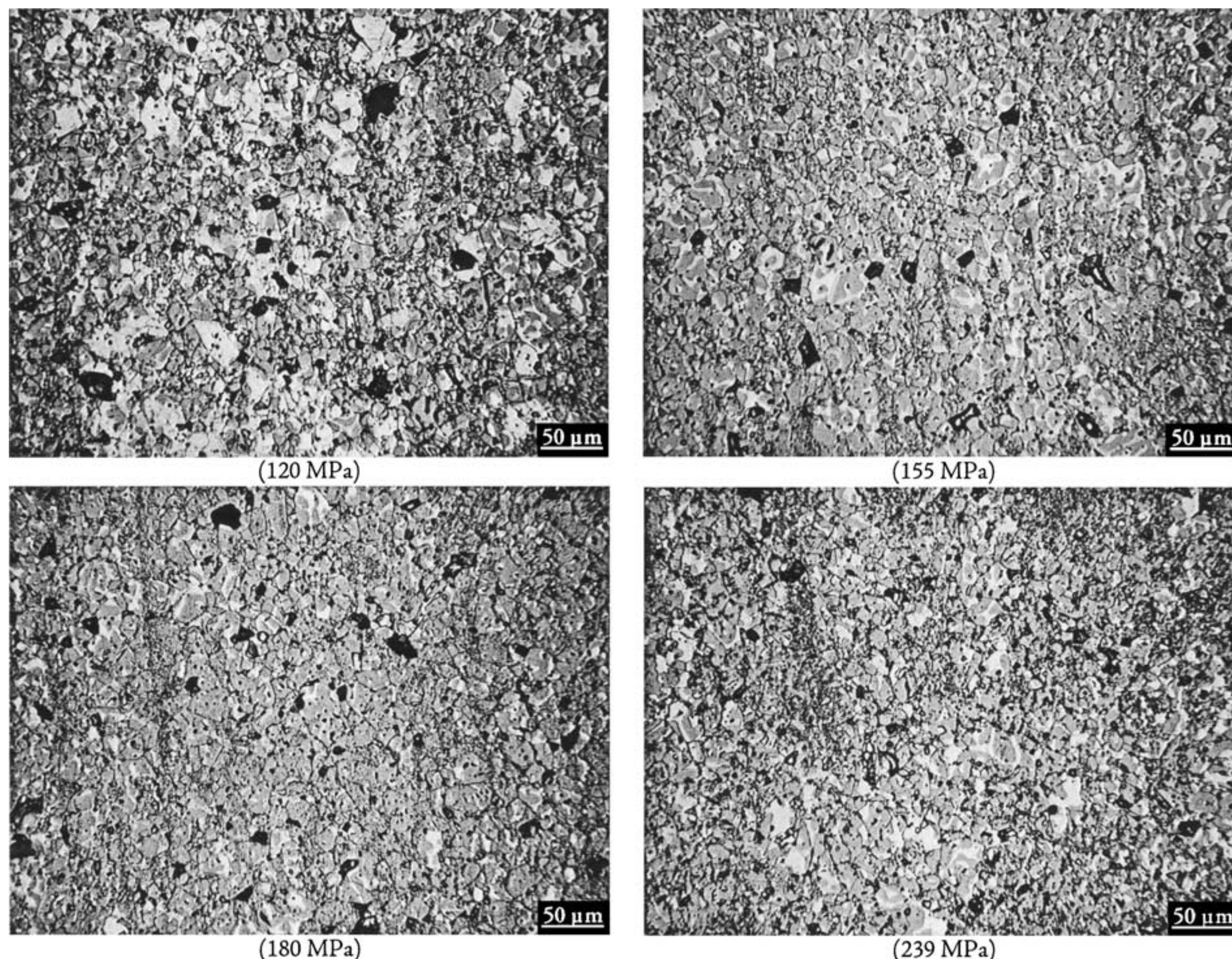

Figure 2 Metal side of fracture surfaces from joints processed at 1150°C in the molybdenum hot press (7.5 MPa). Numbers in parenthesis indicate the failure strength of the beams. The lighter phase is copper; note the correlation between extent of copper film break-up and beam strength.

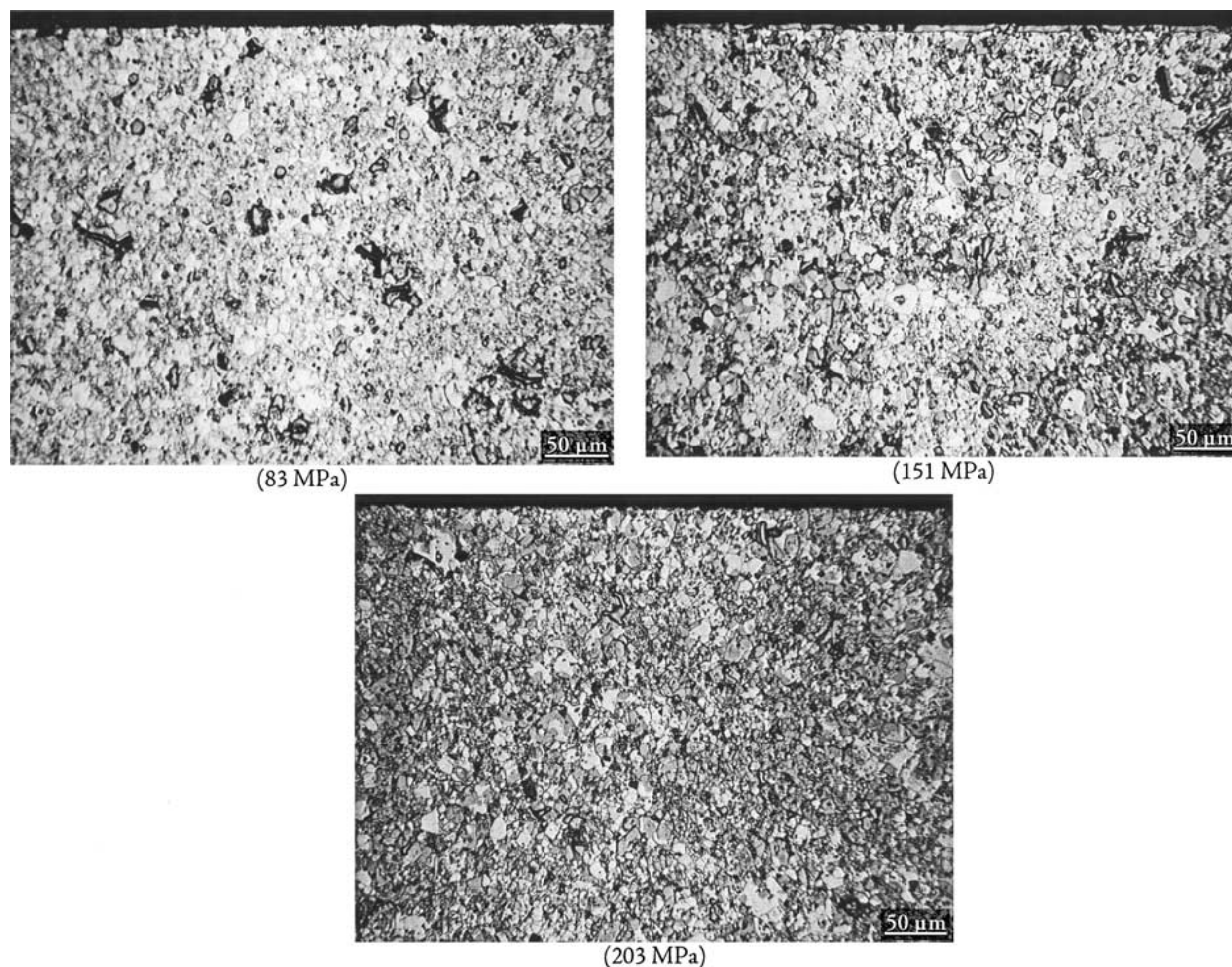

Figure 3 Metal side of fracture surfaces from joints processed at 1150°C in the graphite hot press (2.2 MPa). Numbers in parenthesis indicate the failure strength of the beams. The lighter phase is copper; note the correlation between extent of copper film break-up and beam strength.

the work of adhesion, W_{AD}, for copper/alumina interfaces is expected to be less than that of niobium/alumina interfaces. If the W_{AD} values for the copper-rich and for niobium-rich alloys that develop in the interlayers have similar relative values, the areas of copper/alumina contact represent relatively weaker regions of the interface. When such weaker regions are extensive and in the proximity of interfacial or surface flaws, crack initiation and flaw propagation in these regions may occur at lower applied stress than at or along niobium/alumina contact regions. The reduced stress may also decrease the extent of plastic deformation in the adjoining niobium foil, contributing to a further decrease in the overall work of fracture.

Figs 2 and 3 suggest that the differences in fracture behavior have microstructural origins. As discussed in the Background, the oxygen potential can affect the wetting behavior, interfacial energies, W_{AD}, and thereby work of fracture in metal/alumina systems. The oxygen potential in the two hot pressing environments was expected to differ significantly, and thus, it was initially speculated that these differences in ambient p_{O_2} had exerted a major influence on the resulting fracture behavior. The microstructural differences evident in Figs 2 and 3, and an assessment of copper-oxygen versus niobium-oxygen equilibria suggest that this is unlikely. The p_{O_2} at which niobium is saturated with oxygen (≈3.1 at.% $\underline{O}$) and niobium monoxide forms is on the order of 3×10^{-22} atm at 1150°C. Liquid copper exposed to an ambient p_{O_2} of 3×10^{-22} atm at 1150°C is predicted to have a dissolved oxygen content of ≪1 ppb. Thus, if similar oxygen affinities pertain to the copper-rich and niobium-rich alloys that form during processing, the copper-rich phase in the current study would be expected to contain essentially no oxygen regardless of which of the two hot pressing environments was used. The work of Rühle *et al.* [75] demonstrates that the work of fracture is lower for "pure" copper/alumina interfaces than interfaces between alumina and oxygen-containing copper. Based on this, the extent to which the copper film dewets is the critical issue.

To assess the relative effects of applied pressure versus ambient p_{O_2} on the joint strength characteristics and the interfacial microstructure a third 99.5% alumina joint was prepared at 1150°C in the graphite hot press, in this case with an applied load of 7.5 MPa. Note that the strength statistics for the joint processed in the graphite hot press at 7.5 MPa (192 ± 52 MPa), and those of joints processed in the molybdenum hot press are comparable. As a result of increasing the applied pressure, interfacial microstructures more closely resembling those in Fig. 2 developed. These results suggest that the different ambient p_{O_2} in these two hot presses had at most a minor influence on resulting microstructure and joint strength, and the applied load played the more important role in

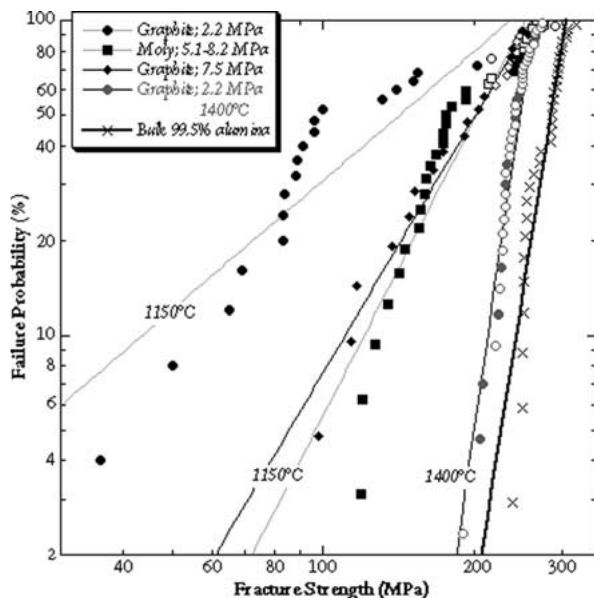

Figure 4 Failure probability plot comparing fracture strength of copper/niobium/copper joints processed under various conditions to the strength of bulk 99.5% alumina. Circles represent data from joints processed at 1150°C in a graphite hot press (2.2 MPa), while squares are for joints processed at 1150°C in a molybdenum hot press (5.1–8.2 MPa). Diamonds represent data from joints processed in the graphite hot press (7.5 MPa). Open symbols are for beams that failed in the ceramic rather than along the metal/ceramic interface.

controlling the resulting strength statistics. The ability to produce stronger joints at 1400°C despite a very low ambient p_{O_2} environment is also consistent with this conclusion.

If the interpretation presented is correct, then variations in strength reflect differences in the severity, spatial density, and interaction among interlayer/alumina interfacial "flaws". The most severe flaws are cracklike voids along the interlayer/alumina interface caused by surface defects in the alumina or foil thickness variations. These interact with one another and/or extensive regions where copper film breakup is incomplete, large regions of copper/alumina persist, and W_{AD} is relatively lower. Since similarly prepared 99.5% aluminas were used, and the amount of liquid formed was essentially the same for bonds prepared at 1150°C and 1400°C, one concludes that higher bonding pressure or higher bonding temperature promote film breakup. Further discussion supporting this view is presented subsequently ¶.

4.2. Effects of processing conditions on interfacial microstructure evolution

For the 99.5% pure alumina, which has been most extensively studied, there is a significant strength increase associated with interfacial dewetting of the copper film. Weak joints developed at 1150°C when small loads (2.2 MPa) were applied, while at higher bonding temperature (1400°C), ceramic failures were prevalent. Temperature and bonding pressure are obviously important.

In a prior study [17], joints were produced at 1400°C (6 h, 2.2 MPa) using sapphire substrates to allow observation of the interfacial microstructure. The interlayer/sapphire interfacial microstructure in these samples exhibited spatial variability. Comparisons of regions at different stages of dewetting suggested the evolution sequence, schematically illustrated in Fig. 5a–c. The initially continuous copper film is disrupted first where asperities in the alumina and niobium surfaces establish point contact with the niobium and alumina, respectively, due to the applied pressure as shown in Fig. 5a. This resembles the early stages of models of interface formation during solid-state diffusion bonding [95–97]. Reimanis [43] noted that during diffusion bonding of pure niobium to sapphire grain boundary groove ridges played a key role in initiating contact formation. Similarly, in the niobium-copper case, grooving of the niobium grain boundaries by the copper liquid creates groove ridges that ultimately contact the alumina surface, Fig. 5b. When the groove ridge along the entire perimeter of a particular niobium

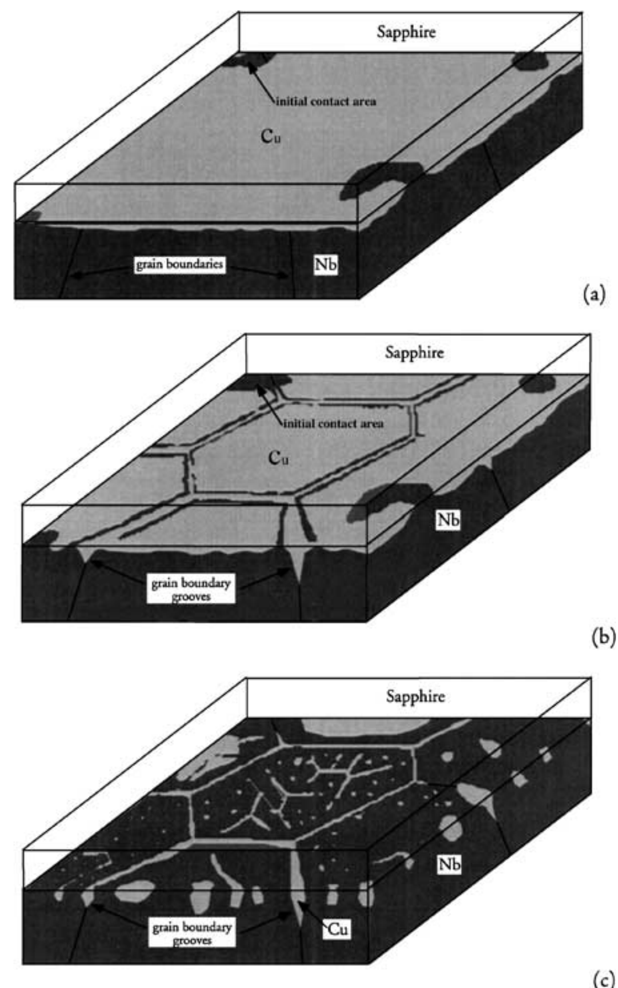

Figure 5 Schematic illustration of the mechanism of liquid copper film break-up. In (a), the film is intact, with niobium/alumina contact only at asperities. In (b), grain boundary grooving and ridging begin to isolate copper atop individual grains. In (c) liquid film instabilities have led to the breakup of the copper film into ligaments or discrete particles.

¶ It has been suggested that the strikingly consistent strength characteristics of bonds formed at 1400°C may in part be due to diminished segregation of interface-weakening impurities as bonding temperature increases. We do not believe this is a factor in the present work. When joints processed at 1400°C were annealed for up to 200 h at 1000°C in vacuum, a time interval expected to be sufficient to allow interfacial segregation, ceramic failures were still observed in room-temperature bend tests [17].

grain contacts the alumina, the liquid copper film is locally isolated, as shown in Fig. 5b. Edge instabilities then ensue, leading to the breakup of these copper patches into copper ligaments. Subsequently, these ligaments undergo Rayleigh instabilities and form discrete droplets of copper, as shown in Fig. 5c. The process resembles that reported by Lange and Clarke [98] for the breakup of an intergranular film in magnesium aluminate spinel ($MgAl_2O_4$) sintered with lithium fluoride additions. Similar morphological changes arise during high-temperature crack healing of sapphire [e.g., 99, 100] and during the break-up of thin solid films, e.g., copper on sapphire during annealing at elevated temperature [60, 63, 67].

An evolution sequence during post-bonding annealing at 1150°C is shown in Fig. 6. The sample was bonded at 1150°C (6 h, 2.2 MPa). Large regions of predominantly copper/sapphire contact remained. Microhardness indents were placed on the sapphire surface to serve as positional reference markers. The sample was then subjected to several anneals at 1150°C (with no externally applied load), and the evolution at selected marked regions of the interface was recorded using optical microscopy. It is clear that there are substantial changes in the interfacial microstructure within 50 h at 1150°C. By comparing the same interface position within the micrograph sequence, evidence for the suggested evolution sequence is obtained. Spatial variability in the evolution may reflect local differences in grain boundary misorientation and grain boundary energy (groove angle) which can affect the grooving kinetics **. Differences in the local values of $\theta_{LC} + \theta_{LM}$ can also contribute to variability, and can additionally lead to redistribution or local depletion of the liquid, or both. In other regions of the interface (not shown) asperities played a more prominent role.

Increases in temperature, and in the applied pressure can be expected to accelerate the breakup of the copper film. The kinetics of evolution dramatically increase when the melting point of copper is exceeded. Interlayer microstructures before and after anneals of ≥400 h duration at 1000°C, below the melting point of copper,

** Local variations in the copper film thickness may also be important and could cause spatial variations in the time required to achieve ridge contact with the alumina. Even submicron variations in the niobium foil thickness can result in important differences in the local copper film thickness, and local film breakup kinetics. At a larger spatial scale, we note that in the two specimens bonded for 6 h at 1150°C at the same applied pressure (2.2 MPa), the weaker sample had a copper coating 3.8 μm thick, and (interfacial) fracture surfaces that were dominated by copper, while the stronger had a 3.0 μm coating and fracture surfaces with more extensive niobium/alumina contact.

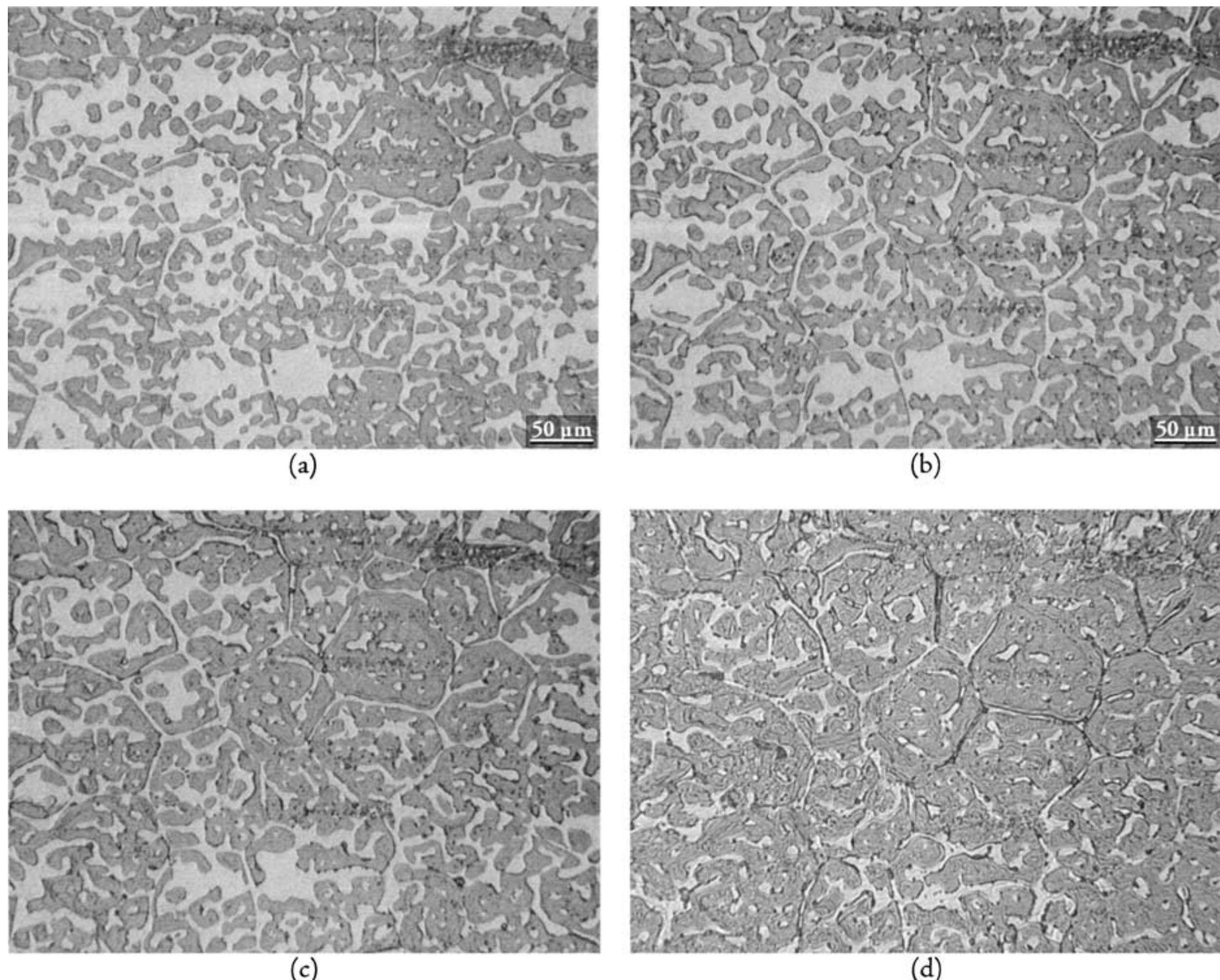

Figure 6 Optical micrographs of the same region of sapphire/interlayer interface after anneals of (a) 15 h, (b) 22 h, (c) 29 h, and (d) 43 h at 1150°C. The lighter grey regions are the Cu phase. Note the initiation of contact along grain boundary groove ridges.

are virtually identical [21]. When transport occurs solely through the solid or along the heterophase interface, the flux is minimal. In contrast, when samples are annealed above the melting point of copper (1085°C), Fig. 6, substantial morphological changes occur in only a few hours. The presence of liquid copper plays a vital role in accelerating the evolution. Diffusion of niobium through the copper liquid is expected to be rapid, and orders of magnitude (perhaps $10^3\times$) faster than solid-state diffusion of niobium through copper. In addition, the solubility of niobium in the copper-rich liquid is on the order of 10–30× higher than in solid copper, and increases with temperature [20]. Thus, more rapid grooving, ridge formation, and niobium redistribution should occur as the temperature increases. Temperature increases will also reduce the flow stress and increase the creep rate of the niobium, contributing to an increased rate of niobium/alumina contact area formation due to foil deformation. In comparing interfacial microstructures of sapphire samples prepared with a constant applied pressure of 2.2 MPa at 1150°C and 1400°C, it is clear that after 6 h film breakup is much more advanced at 1400°C. More complete and uniform film breakup may contribute to the reproducibly high strengths achieved when samples are bonded at 1400°C. Pressure increases are also expected to help bring adjacent noncontacting solid surfaces into closer proximity, allow more irregularities and thermal grooves in the niobium foil to contact the sapphire, and thus accelerate the initial stage of bonding and copper break-up. The higher strength of joints processed at higher pressure at 1150°C would be consistent with this interpretation.

An important characteristic of the evolution is that during dewetting of the copper film, niobium/sapphire or niobium/alumina interface is produced. The liquid copper provides a high diffusivity path for the dissolution and reprecipitation of niobium, and morphological changes occur largely without generation of interfacial voids. The process has similarities to liquid phase sintering, and can be thought of as liquid-phase-assisted diffusion bonding.

When sapphire is replaced with polycrystalline alumina, grooving of the alumina grain boundaries by the liquid metal will occur, and the associated grain boundary groove ridges may also play a role in the evolution. As illustrated in the recent work of Saiz *et al.* [49], grooving occurs more rapidly when the grain boundaries are in contact with liquid than when in contact with vapor. The grooving rate is expected to increase with temperature. The average grain size of the aluminas used is substantially less than that of niobium ($\geq 100\ \mu$m) and thus, alumina grain boundary ridges can be expected to reduce the size of copper patches, and facilitate breakup. Comparisons of interfacial microstructures of sapphire-based and alumina-based joints prepared under similar temperature and applied pressure conditions reveal that the degree of film breakup in the polycrystalline samples is indeed more complete and spatially uniform.

From an energetic perspective, the formation of strong defect-free interfaces hinges upon redistribution of the niobium-saturated copper liquid to eliminate alumina/vapor and niobium/vapor interfaces. It is desirable to have $\gamma_{Cu/Nb} + \gamma_{Cu/Al_2O_3} < \gamma_{Nb} + \gamma_{Al_2O_3}$, where $\gamma_{Cu/Nb}$ and γ_{Cu/Al_2O_3} are the energies of the copper/niobium and copper/alumina interfaces, respectively, and γ_{Nb} and $\gamma_{Al_2O_3}$ are the niobium/vapor and alumina/vapor interfacial energies, respectively. This is equivalent to requiring that the sum of the contact angles of niobium-saturated copper on alumina and on niobium be less than 180°. The combined results of DeLima *et al.* [90], and of Hodkin *et al.* [91] suggest a significant decrease in the contact angle of liquid copper on niobium as the temperature increases from 1090°C to 1500°C. Similar behavior in the present case would allow more complete elimination of interfacial flaws at 1400°C than at 1150°C. Subsequent dewetting of the interlayer/alumina interface and the growth of niobium/alumina contact area requires that the niobium/alumina interfacial energy, γ_{Nb/Al_2O_3}, be less than the sum $\gamma_{Cu/Nb} + \gamma_{Cu/Al_2O_3}$. Extension of this method to other systems would require similar energetics.

4.3. Effect of alumina microstructure on room-temperature strength

Three-quarters of the beams from the 99.5% alumina-based joints processed at 1400°C failed in the ceramic [17]. As a result, the interlayer/alumina interface in these joints must be at least as strong as the 99.5% alumina itself. It was anticipated that by forming joints with progressively stronger aluminas, a transition to interfacial failure might be observed, allowing an assessment of the interfacial strength. In the present study, joints were prepared at 1400°C using both a higher-strength 99.9% alumina, and also using single crystal sapphire. The use of sapphire eliminates the possibility of a glassy phase flowing to and filling interfacial voids, however prior research demonstrates that a glass impurity is not required to form strong interfaces. For example, Dalgleish *et al.* [72] report diffusion-bonded platinum/sapphire joints failed at stresses approaching 1 GPa, and thus, the potential existed for achieving high fracture stresses in the present work. A discussion of the potential dual role of glassy phases on fracture can be found in the study of DeGraaf *et al.* [101].

Preparation of beams from the sapphire-based assembly proved difficult. During the machining of plates, portions of the sample fractured. Only ten beams survived intact; one of these failed during ultrasonic cleaning in acetone. Four beams were tested in the as-bonded condition; the failure strengths varied from 114 to 177 MPa. All four failed at the interface, and the "average" fracture strength (142 ± 29 MPa) was less than that of similarly processed 99.5% alumina joints. The remaining five beams were annealed for 10 h in vacuum at 1400°C prior to testing. It was expected that such anneals would result in more complete breakup of the copper film, and might promote healing of any near-interfacial flaws that developed during machining. These five annealed beams all failed at the interface, at stresses that ranged from 110 to 253 MPa. Although the annealing increased the average strength (185 ± 60 MPa), the statistics are poor.

Examination of the fracture surfaces of as-processed sapphire beams showed regions in which copper patches >100 μm in size persisted. In other regions the film had locally dewetted the interface but copper ligaments remain interconnected over dimensions >500 μm. Unbonded regions are also evident, but the unbonded area fraction is comparable to that in 99.5% alumina beams that also failed along the interlayer/alumina interface but generally at higher applied stresses. The results suggest a higher interfacial fracture resistance in the polycrystalline materials, perhaps because of the interface topography. Lithography and ion beam etching may be useful in producing sapphire substrates with controlled surface topography. The relationship between interfacial microstructure and strength characteristics is discussed further in the subsequent section.

Joints produced using 99.9% alumina had a higher average fracture strength than comparably processed 99.5% alumina. A limited amount of the 99.9% material was available for joining and testing. All five beams tested at room temperature failed in the ceramic. The average strength, 359 MPa, exceeds that for the 99.5% material, and the standard deviation (±26 MPa) is small. The average bend strength of beams prepared from as-received 99.9% alumina material is ≈560 MPa, and thus, the bonded-beam strength is only ≈65% that of the as-received ceramic. Grain growth during the bonding cycle (6 h, 1400°C) is likely to contribute to this strength decrease. After thermal etching (45 min, 1350°C), the mean linear intercepts in "as-received" and bonded 99.9% alumina were ≈0.9 and ≈1.2 μm, respectively. Seidel *et al.* [102] examined the grain size dependence of the fracture strength of a similarly high-purity high-density alumina. Within the grain size range of 1.7 to 11 μm, a roughly linear relationship between strength and the inverse square root of grain size is indicated. Similar trends in the present material would account for ≈40% of the observed strength decrease.

4.4. High-temperature strength and failure mode

The remaining fourteen beams from the 99.9% alumina joint were mechanically tested at elevated temperature. Fig. 7 compares the temperature dependence of the fracture strength for this joint with that of a 99.5% alumina joint processed at 1400°C [17]. Although the strength improvement at room temperature is modest, the superiority of joints prepared with the 99.9% alumina becomes evident at higher temperatures. Above 900°C, the strength of the 99.5% alumina beams drops off rather sharply, while failures still occur in the ceramic. In the 99.9% alumina joint, ceramic failures are also observed up to 1100°C, but they occur at substantially higher stress. At 1200°C, the four beams tested failed at the interface within a narrow strength range

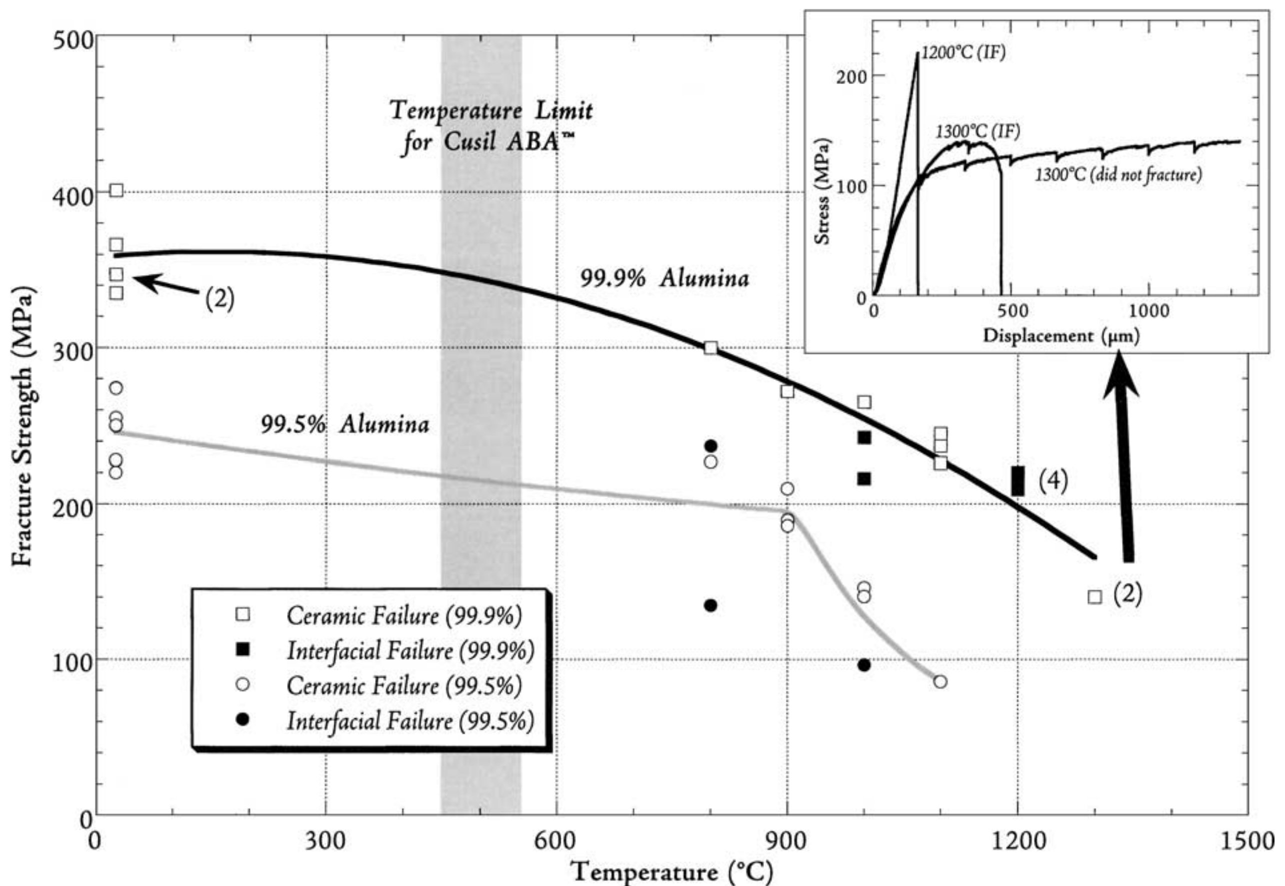

Figure 7 Fracture strength versus temperature for 99.5% and 99.9% alumina joints processed at 1400°C. Numbers in parenthesis indicate the number of overlapping data points. Beams tested at 1300°C underwent creep as indicated by the inserted stress versus displacement curves. The slope of the curve at 1200°C is representative of those from tests performed at lower temperatures as well.

(209–220 MPa). In the two beams tested at 1300°C, the alumina and niobium undergo plastic deformation, as illustrated by the stress-displacement curve inserts in Fig. 7. The area fraction of niobium/alumina contact is apparently sufficiently high that the remelting of the residual copper and the formation of small liquid droplets along the interface does not seriously degrade the strength.

The majority of room-temperature fractures in beams from assemblies processed at 1400°C initiate and propagate entirely within the ceramic. Similar trends persist as the test temperature is increased. Thus, the interlayer/alumina interfaces formed in both the 99.5% and 99.9% alumina joints are sufficiently strong for joining these particular aluminas. The relative strengths of interfaces formed between the interlayer and the

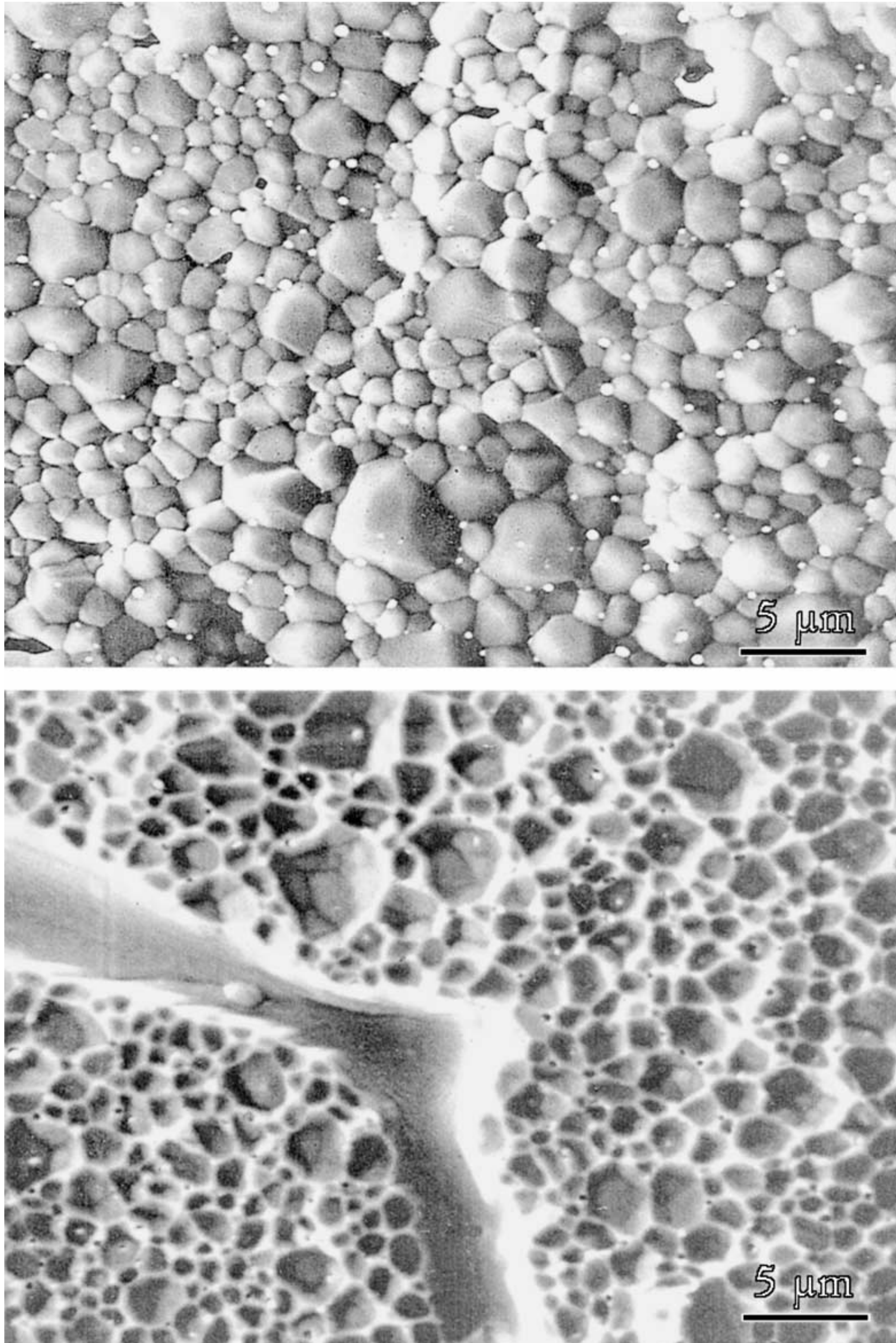

Figure 8 SEM micrographs of the ceramic (top) and metal (bottom) side of a fracture surface in the 99.9% alumina joint. Note the facetting of the alumina and the roughness of the interface.

99.5% versus 99.9% alumina is uncertain. However, the more homogeneous and finer grain size microstructure of the 99.9% alumina, and the relatively smaller flaw (void/pore) size, should translate into smaller and less damaging interfacial voids. The weakest 99.5% alumina beams tested at high temperature (see 800°C and 1000°C in Fig. 7) are characterized by large unbonded networks at the interface, while only a few isolated and small unbonded regions developed in the 99.9% alumina joint.

4.5. Effects of alumina microstructure on interfacial (joint) microstructural evolution

Joints using three different aluminum oxide substrates (Coors AD995, Nikkato SSW-999W, and single crystal sapphire) exhibit distinct ceramic/interlayer interfacial microstructures and distinct fracture characteristics. When highly polished single-crystal (0001) sapphire substrates are used there is generally variability in the extent of copper film breakup; this variability is accentuated when the bonding temperature and pressure are decreased. In the coarser grain size 99.5% alumina, the copper film is broken up completely at 1400°C, and again, decreases in temperature and bonding pressure lead to less complete and homogeneous breakup. The joint fabricated with the finest grain size material, the 99.9% alumina, revealed very few interfacial copper particles of large enough size to be observed with an optical microscope. The copper was subsequently observed as round particles (<0.5 μm) at alumina grain boundaries via SEM (see Fig. 8). Note also the pronounced facetting of the alumina, the roughness of the ceramic fracture surface, and the corresponding roughness on the metal fracture surface. The decreased wavelength of the interfacial roughness relative to the 99.5% material, and possibly a higher amplitude of roughness, increase the surface area produced during interfacial fracture, and force an interfacial crack to be redirected.

Collectively, the results point to the important role that grooving of alumina grain boundaries, and/or facetting of the alumina itself can have on copper redistribution, film breakup and the ultimate interfacial microstructure. Relative to single crystals, the polycrystalline materials will have a greater spatial variation in the driving forces and kinetics for grain boundary grooving and film break-up. However, the ceramic grain boundaries appear to play a role in reducing the spatial scale of fluctuations in the copper film to periodicities smaller than the niobium grain size. Regions of copper at the metal/ceramic interface that are smaller than the 99.5% alumina grain size (<25 μm) and widely separated are likely to be sufficiently small that they are not of critical size for failure initiation. (Indeed, we note that when the copper is present as ligaments that are fine in one dimension, or is in the form of small discrete particles, interfacial cracks deviate into and tear the copper. It is only when the copper is present in the form of larger patches that the failure propagates along the copper/alumina interface.) Copper diffusion along niobium grain boundaries may lead to some copper loss from the interface, and contribute to copper depletion from selected niobium grain boundary grooves. There is also some microstructural evidence suggesting that for the finest grain size material, copper diffusion into the alumina may also reduce the total amount of copper second phase along the interface. Consequently, polycrystalline joints are more likely to have strong interfaces, enabling preferential failure in the ceramic, as observed in such joints processed at 1400°C.

5. Conclusions

Multilayer copper/niobium/copper interlayers provided an effective means of joining alumina ceramics. The fracture characteristics of the joints were sensitive to the alumina/interlayer microstructure developed during processing. The nature of this microstructure hinged, in turn, upon the processing conditions used, and the microstructure of the alumina selected. Dewetting of the initially continuous copper films, the formation of discrete copper droplets (particles), and the concurrent increase of alumina/niobium contact area were identified as key aspects of interfacial microstructure evolution. Increases in bonding pressure at fixed temperature, and increases in bonding temperature at fixed pressure improved the strength characteristics. Studies of fracture surfaces indicated that joints with a large copper/alumina interfacial area fraction were comparatively weak, and suggested a correlation between increased joint strengths and an increased degree and uniformity of copper film break-up. As fracture strengths increased, failures tended to shift from the alumina/interlayer interface to the ceramic, and fracture strengths were ultimately limited by the strength of the ceramic. The alumina/interlayer microstructure and joint properties were also sensitive to the microstructure of the alumina joined. Joints processed at 1400°C using fine grain size alumina exhibited the best room-temperature strength characteristics. When a high area fraction of alumina/niobium contact was achieved, joints retained useful levels of strength to temperatures above the melting point of copper.

More generally, the results indicate that strong and refractory joints can be produced using multilayer interlayers in which the layer components do not exhibit significant mutual solubility. The success of the method hinges on interfacial energetics that (initially) promote void filling by the liquid, but ultimately favor the growth of solid-solid interfaces and interfacial dewetting of the liquid film. If such conditions are widely met, the joining approach may substantially expand the range of interlayer constituents and designs that can be considered for the fabrication of refractory joints.

Acknowledgements

This research was supported by the Director, the Office of Energy Research, Office of Basic Energy Sciences, Materials Sciences Division of the U.S. Department of Energy under Contract No. DE-AC03-76SF00098. The authors thank Professor Kunihiko Nakashima for providing the high-strength alumina. A. M. Glaeser especially thanks the faculty and staff of the Laboratory

for Solid-State Chemistry and Materials Science at the Technical University of Eindhoven, The Netherlands, for their warm hospitality during the preparation of this manuscript. Dr. A. Kodentsov, Professor F. van Loo, Professor B. De With and Dr. John R. Smith are thanked for helpful discussions and communications regarding ceramic/metal interfaces.

References

1. M. G. NICHOLAS and D. A. MORTIMER, *Mater. Sci. Tech.* **1**(9) (1985) 657.
2. K. SUGANUMA, Y. MIYAMOTO and M. KOIZUMI, *Ann. Rev. Mater. Sci.* **18** (1988) 33.
3. R. E. LOEHMAN and A. P. TOMSIA, *Am. Ceram. Soc. Bull.* **67**(2) (1988) 375.
4. G. ELSSNER and G. PETZOW, *ISIJ Int.* **30**(12) (1990) 1011.
5. M. G. NICHOLAS, "Joining of Ceramics," 1st ed. (Chapman and Hall, London, New York, 1990).
6. R. V. ALLEN and W. E. BORBIDGE, *J. Mater. Sci.* **18**(9) (1983) 2835.
7. Y. IINO, *J. Mater. Sci. Lett.* **10**(2) (1991) 104.
8. M. L. SHALZ, B. J. DALGLEISH, A. P. TOMSIA and A. M. GLAESER, *J. Mater. Sci.* **28**(6) (1993) 1673.
9. *Idem.*, *ibid.* **29**(12) (1994) 3200.
10. M. L. SHALZ, B. J. DALGLEISH, A. P. TOMSIA, R. M. CANNON and A. M. GLAESER, *ibid.* **29**(14) (1994) 3678.
11. B. J. DALGLEISH, A. P. TOMSIA, K. NAKASHIMA, M. R. LOCATELLI and A. M. GLAESER, *Scripta Metall. Mater.* **31**(8) (1994) 1043.
12. M. R. LOCATELLI, A. P. TOMSIA, K. NAKASHIMA, B. J. DALGLEISH and A. M. GLAESER, *Key Eng. Mater.* **111/112** (1995) 157.
13. G. CECCONE, M. G. NICHOLAS, S. D. PETEVES, A. P. TOMSIA, B. J. DALGLEISH and A. M. GLAESER, *Acta Mater.* **44**(2) (1996) 657.
14. B. J. DALGLEISH, K. NAKASHIMA, M. R. LOCATELLI, A. P. TOMSIA and A. M. GLAESER, *Ceram. Int.* **23**(4) (1997) 313.
15. M. PAULASTO, G. CECCONE and S. D. PETEVES, *Scripta Mater.* **36**(10) (1997) 1167.
16. S. D. PETEVES, M. PAULASTO, G. CECCONE and V. STAMOS, *Acta Mater.* **46**(7) (1998) 2407.
17. R. A. MARKS, D. R. CHAPMAN, D. T. DANIELSON and A. M. GLAESER, *ibid.* **48**(18-19) (2000) 4425.
18. L. BERNSTEIN and H. BARTHOLOMEW, *Trans. AIME* **236**(3) (1966) 405.
19. D. S. DUVALL, W. A. OWCZARSKI and D. F. PAULONIS, *Welding Journal* **53**(4) (1974) 203.
20. T. B. MASSALSKI, H. OKAMOTO and ASM International, "Binary Alloy Phase Diagrams," 2nd ed. (ASM International, Materials Park, Ohio, 1990).
21. R. A. MARKS, M.S. thesis, Department of Materials Science and Mineral Engineering, University of California, Berkeley, 2000.
22. M. KUWABARA, J. C. H. SPENCE and M. RÜHLE, *J. Mater. Res.* **4**(4) (1989) 972.
23. W. MADER, *Z. Metallkde.* **80**(3) (1989) 139.
24. K. M. KNOWLES, K. B. ALEXANDER, R. E. SOMEKH and W. M. STOBBS, *Inst. Phys. Conf. Ser.* **90** (1987) 245.
25. F. S. OHUCHI, *J. Mater. Sci. Lett.* **8**(12) (1989) 1427.
26. J. MAYER, C. P. FLYNN and M. RÜHLE, *Ultramicroscopy* **33**(1) (1990) 51.
27. J. MAYER, J. A. DURA, C. P. FLYNN and M. RÜHLE, *Surface and Coatings Technology* **43/44**(1) (1990) 199.
28. V. GUPTA, J. WU and A. N. PRONIN, *J. Amer. Ceram. Soc.* **80**(12) (1997) 3172.
29. F. S. OHUCHI and M. KOHYAMA, *ibid.* **74**(6) (1991) 1163.
30. G. ELSSNER, S. RIEDEL and R. PABST, *Prakt. Metall.* **12** (1975) 234.
31. S. MOROZUMI, M. KIKUCHI and T. NISHINO, *J. Mater. Sci.* **16**(8) (1981) 2137.
32. M. TURWITT, G. ELSSNER and G. PETZOW, *J. de Physique* **46** (Supplement C4) (1985) 123.
33. B. GIBBESCH, G. ELSSNER, W. MADER and H. F. FISCHMEISTER, in "Joining Ceramics, Glass, and Metal," edited by W. Kraft and Deutsche Gesellschaft für Metallkunde, (DGM Informationsgesellschaft, Oberursel, 1989) p. 65.
34. *Idem.*, *Ceram. Eng. Sci. Proc.* **10**(11/12) (1989) 1503.
35. D. KORN, G. ELSSNER, H. F. FISCHMEISTER and M. RÜHLE, *Acta Metall. Mater.* **40** (Supplement) (1992) S355.
36. G. ELSSNER, D. KORN and M. RÜHLE, *Scripta Metall. Mater.* **31**(8) (1994) 1037.
37. G. SOYEZ, G. ELSSNER, M. RÜHLE and R. RAJ, *Acta Mater.* **46**(10) (1998) 3571.
38. M. RÜHLE, K. BURGER and W. MADER, *J. Microsc. Spectrosc. Electron. (France)* **11** (1986) 163.
39. M. RÜHLE, M. BACKHAUS-RICOULT, K. BURGER and W. MADER, in "Ceramic Microstructures '86," edited by J. A. Pask and A. G. Evans (Plenum Press, New York, 1987) p. 295.
40. K. BURGER, W. MADER and M. RÜHLE, *Ultramicroscopy*, **22** (1987) 1.
41. K. BURGER and M. RÜHLE, *Ceram. Eng. Sci. Proc.* **10**(11–12) (1989) 1549.
42. *Idem.*, *Ultramicroscopy* **29**(1–4) (1989) 88.
43. I. E. REIMANIS, *Acta Metall. Mater.* **40** (Supplement) (1992) S67.
44. M. FLORJANCIC, W. MADER, M. RÜHLE and M. TURWITT, *J. de Physique* **46** (Supplement C4) (1985) 129.
45. W. MADER and M. RÜHLE, *Acta Metall.* **37**(3) (1989) 853.
46. D. KNAUSS and W. MADER, *Ultramicroscopy* **37**(1-4) (1991) 247.
47. G. ELSSNER and G. PETZOW, *Z. Metallkde.* **64**(4) (1973) 280.
48. E. SAIZ, A. P. TOMSIA and R. M. CANNON, in "Ceramic Microstructures: Control at the Atomic Level," edited by A. P. Tomsia and A. M. Glaeser (Plenum Press, New York, 1998), p. 65.
49. E. SAIZ, R. M. CANNON and A. P. TOMSIA, *Acta Mater.* **47**(15) (1999) 4209.
50. M. BACKHAUS-RICOULT and S. LAURENT, in "Interfacial Science in Ceramic Joining," edited by A. Bellosi, T. Kosmac and A. P. Tomsia (Kluwer Academic Publishers, Dordrecht, The Netherlands, 1998) p. 169.
51. I. G. BATIREV, A. ALAVI and M. W. FINNIS, *Phys. Rev. B* **62**(7) (2000) 4698.
52. I. G. BATIREV, A. ALAVI, M. W. FINNIS and T. DEUTSCH, *Phys. Rev. Lett.* **82**(7) (1999) 1510.
53. W. ZHANG and J. R. SMITH, *Phys. Rev. B* **61**(24) (2000) 16883.
54. I. BATYREV, A. ALAVI and M. W. FINNIS, *Faraday Discuss.* **114**(1) (1999) 33.
55. H. F. FISCHMEISTER, W. MADER, B. GIBBESCH and G. ELSSNER, in "Interfacial Structure, Properties and Design," vol. 122, edited by W. A. T. Clark, C. L. Briant and M. H. Yoo (Materials Research Society, Pittsburgh, PA, 1988) p. 529.
56. C. J. MCMAHON, JR. and V. VITEK, *Acta Metall.* **27**(4) (1979) 507.
57. G. ELSSNER and U. KROHN, *Z. Metallkde.* **70**(2) (1979) 71.
58. J. T. KLOMP, in "Ceramic Microstructures '86," edited by J. A. Pask and A. G. Evans (Plenum Press, New York, 1987) p. 307.
59. F. ERNST, P. PIROUZ and A. H. HEUER, *Philos. Mag. A* **63**(2) (1991) 259.
60. R. M. PILLIAR and J. NUTTING, *ibid.* **16**(139) (1967) 181.
61. F. S. OHUCHI, R. H. FRENCH and R. V. KASOWSKI, *J. Appl. Phys.* **62**(6) (1987) 2286.
62. R. V. KASOWSKI, F. S. OHUCHI and R. H. FRENCH, *Physica B* **150**(1) (1988) 44.
63. C. M. KENNEFICK and R. RAJ, *Acta Metall.* **37**(11) (1989) 2947.
64. M. GAUTIER, J. P. DURAUD and L. PHAM VAN, *Surface Science* **249**(1-3) (1991) L327.
65. Q. GUO and P. J. MOLLER, *ibid.* **244**(3) (1991) 228.
66. G. DEHM, M. RUHLE, G. DING and R. RAJ, *Philos. Mag. B* **71**(6) (1995) 1111.
67. A. SOPER, B. GILLES and N. EUSTATHOPOULOS, *Mater. Sci. Forum* **207–209** (1996) 433.
68. C. A. M. MULDER and J. T. KLOMP, *J. de Physique* **46** (Supplement C4) (1985) 111.

69. C. BERAUD, M. COURBIERE, C. ESNOUF, D. JUVE and D. TREHEUX, *J. Mater. Sci.* **24**(12) (1989) 4545.
70. R. M. CRISPIN and M. G. NICHOLAS, *Cream. Eng. Sci. Proc.* **10**(11/12) (1989) 1575.
71. B. GIBBESCH and G. ELSSNER, *Acta Metall. Mater.* **40** (Supplement) (1992) S59.
72. B. J. DALGLEISH, E. SAIZ, A. P. TOMSIA, R. M. CANNON and R. O. RITCHIE, *Scripta Metall. Mater.* **31**(8) (1994) 1109.
73. K. A. ROGERS, K. P. TRUMBLE, B. J. DALGLEISH and I. E. REIMANIS, *J. Amer. Ceram. Soc.* **77**(8) (1994) 2036.
74. L. ESPOSITO, A. BELLOSI, S. GUICCIARDI and G. DE PORTU, *J. Mater. Sci.* **33**(7) (1998) 1827.
75. M. RÜHLE, A. LIEDTKE, U. ALBER, R. SCHWEINFEST and G. ELSSNER, in "Interfacial Science in Ceramic Joining," edited by A. Bellosi, T. Kosmac and A. P. Tomsia (Kluwer Academic Publishers, Dordrecht, The Netherlands, 1998) p. 3.
76. G. L. ZHAO, J. R. SMITH, J. RAYNOLDS and D. J. SROLOVITZ, *Interface Science* **3**(4) (1996) 289.
77. I. E. REIMANIS, K. P. TRUMBLE, K. A. ROGERS and B. J. DALGLEISH, *J. Amer. Ceram. Soc.* **80**(2) (1997) 424.
78. T. E. O'BRIEN and A. C. D. CHAKLADER, *ibid.* **57**(8) (1974) 329.
79. S. P. MEHROTRA and A. C. D. CHAKLADER, *Metall. Trans. B* **16B**(9) (1985) 567.
80. J. V. NAIDICH, in "Progress in Surface and Membrane Science," edited by D. A. Cadenhead and J. F. Danielli (Academic Press, London, 1981) p. 353.
81. V. GHETTA, J. FOULETIER and D. CHATAIN, *Acta Mater.* **44**(5) (1996) 1927.
82. Y. V. NAIDICH and V. S. ZHURAVLEV, *Refractories (USSR)* **15**(1/2) (1974) 55.
83. P. KRITSALIS, L. COUDURIER and N. EUSTATHOPOULOS, *J. Mater. Sci.* **26**(12) (1991) 3400.
84. P. KRITSALIS, J. G. LI, L. COUDURIER and N. EUSTATHOPOULOS, *J. Mater. Sci. Lett.* **9**(11) (1990) 1332.
85. A. P. TOMSIA, E. SAIZ, S. FOPPIANO and R. M. CANNON, in Proc. Int. Conf. High Temperature Capillarity, edited by N. Eustathopoulos and N. Sobczak, Cracow, Poland, 1997, p. 59.
86. M. NICHOLAS, R. R. D. FORGAN and D. M. POOLE, *J. Mater. Sci.* **3**(1) (1968) 9.
87. K. NOGI, K. OISHI and K. OGINO, *Mater. Trans. JIM* **30**(2) (1989) 137.
88. P. NIKOLOPOULOS, S. AGATHOPOULOS and A. TSOGA, *J. Mater. Sci.* **29**(16) (1994) 4393.
89. J.-G. LI, *J. Amer. Ceram. Soc.* **75**(11) (1992) 3118.
90. O. F. DE LIMA, M. KREHL and K. SCHULZE, *J. Mater. Sci.* **20**(7) (1985) 2464.
91. E. N. HODKIN, M. G. NICHOLAS and D. M. POOLE, *J. Less-Common Metals* **20**(2) (1970) 93.
92. E. SAIZ, R. M. CANNON and A. P. TOMSIA, unpublished work.
93. J. KRUZIC, R. A. MARKS, A. M. GLAESER and R. O. RITCHIE, unpublished work.
94. J. MCKEOWN, unpublished work.
95. B. DERBY and E. R. WALLACH, *Metal Science* **16**(1) (1982) 49.
96. *Idem.*, *ibid.* **18**(9) (1984) 427.
97. A. HILL and E. R. WALLACH, *Acta Metall.* **37**(9) (1989) 2425.
98. F. F. LANGE and D. R. CLARKE, *J. Amer. Ceram. Soc.* **65**(10) (1982) 502.
99. J. RÖDEL and A. M. GLAESER, *ibid.* **73**(3) (1990) 592.
100. J. D. POWERS and A. M. GLAESER, *ibid.* **75**(9) (1992) 2547.
101. M. DE GRAEF, B. J. DALGLEISH, M. R. TURNER and A. G. EVANS, *Acta Metall. Mater.* **40** (Supplement) (1992) S333.
102. J. SEIDEL, N. CLAUSSEN and J. RÖDEL, *J. Eur. Ceram. Soc.* **15**(5) (1995) 395.

Received 21 September 2000
and accepted 11 May 2001